https://doi.org/10.5194/nhess-2019-182
Preprint. Discussion started: 20 June 2019

Natural Hazards and Earth System Sciences
Discussions

Nonlinear deformation and run-up of single tsunami waves of positive polarity: numerical simulations and analytical predictions

Ahmed A. Abdalazeez [1], Ira Didenkulova [1, 2], Denys Dutykh [3]

[1] Department of Marine Systems, Tallinn University of Technology, Akadeemia tee 15A, Tallinn 12618, Estonia
[2] Nizhny Novgorod State Technical University n.a. R.E. Alekseev, Minin str. 24, Nizhny Novgorod 603950, Russia
[3] Univ. Grenoble Alpes, Univ. Savoie Mont Blanc, CNRS, LAMA, Chambéry, 73000, France

Correspondence to: Ahmed A. Abdalazeez (ahabda@ttu.ee)

Abstract. The estimate of individual wave run-up is especially important for tsunami warning and risk assessment as it allows to evaluate the inundation area. Here as a model of tsunami we use the long single wave of positive polarity. The period of such wave is rather long which makes it different from the famous Korteweg-de Vries soliton. This wave is nonlinearly deformed during its propagation in the ocean, which results in a steep wave front formation. Situations, when waves approach the coast with a steep front are often observed during large tsunamis, e.g. 2004 Indian Ocean and 2011 Tohoku tsunamis. Here we study the nonlinear deformation and run-up of long single waves of positive polarity in the conjoined water basin, which consists of the constant depth section and a plane beach. The work is performed numerically and analytically in the framework of the nonlinear shallow water theory. Analytically, wave propagation along the constant depth section and its run-up on a beach are considered independently without taking into account wave reflection from the toe of the bottom slope. The propagation along the bottom of constant depth is described by Riemann wave, while the wave run-up on a plane beach is calculated using rigorous analytical solutions of the nonlinear shallow water theory following the Carrier-Greenspan approach. Numerically, we use the finite volume method with the second order UNO2 reconstruction in space and the third order Runge-Kutta scheme with locally adaptive time steps. During wave propagation along the constant depth section, the wave becomes asymmetric with a steep wave front. Shown, that the maximum run-up height depends on the front steepness of the incoming wave approaching the toe of the bottom slope. The corresponding formula for maximum run-up height which takes into account the wave front steepness is proposed.

1. Introduction

Evaluation of wave run-up characteristics is one of the most important tasks in coastal oceanography especially when estimating tsunami hazard. This knowledge is required as for planning coastal structures and protection works, as for short-term tsunami forecast and tsunami warning. Its importance is also confirmed by a number of scientific papers, see recent works (Tang et al. 2017; Touhami and Khellaf 2017; Zainali et al. 2017; Raz et al. 2018; Yao et al. 2018).

https://doi.org/10.5194/nhess-2019-182
Preprint. Discussion started: 20 June 2019


Natural Hazards and Earth System Sciences
Discussions

The general solution of the nonlinear shallow water equations on a plane beach was found by Carrier and Greenspan (1958) using the hodograph transformation. Later on many other authors found specific solutions for different types of waves climbing the beach, see, for instance, (Pedersen and Gjevik 1983; Synolakis 1987; Synolakis et al. 1988; Mazova et al. 1991; Pelinovsky and Mazova 1992; Tadepalli and Synolakis 1994; Brocchini and Gentile 2001; Carrier et al. 2003; Kânoglu 2004; Tinti and Tonini 2005; Kânoglu and Synolakis 2006; Madsen and Fuhrman 2008; Didenkulova et al. 2007; Didenkulova 2009; Madsen and Schaffer 2010).

It is worth mentioning that many analytical formulas have been validated experimentally in laboratory tanks (Synolakis 1987, Li and Raichlen 2002; Lin et al. 2009; Didenkulova et al. 2013). For most of them, the solitary waves have been used. The soliton is rather easy to generate in the flume, therefore, laboratory studies of run-up of solitons are the most popular. However, (Madsen et al. 2008) pointed out that the solitons are inappropriate to describe the real tsunami and proposed to use waves of longer duration than solitons and downscaled records of real tsunami. Schimmels et al. (2016) and Sriram et al. (2016) generated such long waves in the Large Wave Flume of Hannover (GWK FZK) using the piston type of wave maker while McGovern et al. (2018) did it using the pneumatic wave generator. In this paper, we study the nonlinear deformation and run-up of such long single pulses of positive polarity on a plane beach.

A similar study was performed for periodic sine waves (Didenkulova et al. 2007; Didenkulova 2009). It was shown that the run-up height increases with an increase in the wave asymmetry (wave front steepness) which is a result of nonlinear wave deformation during its propagation in a basin of constant depth. It was found analytically that the run-up height of this nonlinearly deformed sine wave is proportional to the square root of the wave front steepness. Later on, this result was also confirmed experimentally (Didenkulova et al. 2013).

It should be noted that these analytical finding also match tsunami observations. Steep tsunami waves are often witnessed and reported during large tsunami events, such as 2004 Indian Ocean and 2011 Tohoku tsunamis. Sometimes the wave which approaches the coast represents a “wall of water” or a bore, which is demonstrated by numerous photos and videos of these events.

The nonlinear steepening of the long single waves of positive polarity has also been observed experimentally in (Sriram et al. 2016), but its effect on wave run-up has not been studied yet. In this paper, we study this effect both analytically and numerically. Analytically, we apply the methodology developed in (Didenkulova 2009; Didenkulova et al. 2014), where we consider the processes of wave propagation in the basin of constant depth and the following wave run-up on a plane beach independently, not taking into account the point of merging of these two bathymetries. Numerically, we solve the nonlinear shallow water equations.

The paper is organized as follows. In Section 2, we give the main formulas and briefly describe the analytical solution. The numerical model is described and validated in Section 3. The nonlinear deformation and run-up of the long single wave of positive polarity is described in Section 4. The main results are summarized in Section 5.

https://doi.org/10.5194/nhess-2019-182
Preprint. Discussion started: 20 June 2019

Natural Hazards and Earth System Sciences
Discussions

2. Analytical solution

We solve the nonlinear shallow water equations for the bathymetry shown in Fig. 1:

$$\frac{\partial u}{\partial t} + u\frac{\partial u}{\partial x} + g\frac{\partial \eta}{\partial x} = 0\,, \tag{1}$$

$$\frac{\partial \eta}{\partial t} + \frac{\partial}{\partial x}\left[\left(h(x)+\eta\right)u\right] = 0\,. \tag{2}$$

Here $\eta(x, t)$ is the vertical displacement of the water surface with respect to the still water level, $u(x,t)$ – depth-averaged water flow, $h(x)$ – unperturbed water depth, g is the gravitational acceleration, x is the coordinate directed onshore, and t is time. The system of Eqs.(1),(2) is solved independently for the two bathymetries shown in Fig. 1: a basin of constant depth h_0 and length X_0 and a plane beach, where the water depth $h(x) = -x\tan\alpha$.

Eqs. (1),(2) can be solved exactly for a few specific cases. In the case of constant depth, the solution is described by the Riemann wave (Stoker 1957). Its adaptation for the boundary problem can be found in Zahibo et al. (2008). In the case of a plane beach, the corresponding solution was found by Carrier and Greenspan (1958). Both solutions are well-known and widely used and we do not reproduce them here, but just provide some key formulas.

As already mentioned, during its propagation along the basin of constant depth h_0, the wave transforms as a Riemann wave (Zahibo et al. 2008):

$$\eta(x,t) = \eta_0\left[t - \frac{x + X_0 + L}{V(x,t)}\right], \tag{3}$$

$$V(x,t) = 3\sqrt{g\left[h_0 + \eta(x,t)\right]} - 2\sqrt{gh_0}\,, \tag{4}$$

where $\eta_0(x = -L - X_0, t)$ is the water displacement at the left boundary. After the propagation over the section of constant depth h_0, the incident wave has the following shape:

$$\eta_{X0}(t) = \eta_0\left[t - \frac{X_0}{V(x,t)}\right], \qquad V_{X0}(t) = 3\sqrt{g\left[h_0 + \eta_{X0}(t)\right]} - 2\sqrt{gh_0}\,. \tag{5}$$

Following the methodology developed in Didenkulova (2008), we let this nonlinearly deformed wave described by Eq. (5) run-up on a plane beach, characterized by the water depth $h(x) = -x\tan\alpha$. This approach does not take into account the merging point of the two bathymetries and, therefore, does not account for reflection from the toe of the slope and wave interaction with the reflected wave.

https://doi.org/10.5194/nhess-2019-182
Preprint. Discussion started: 20 June 2019

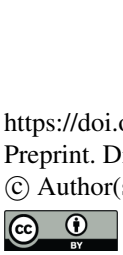

Natural Hazards and Earth System Sciences
Discussions

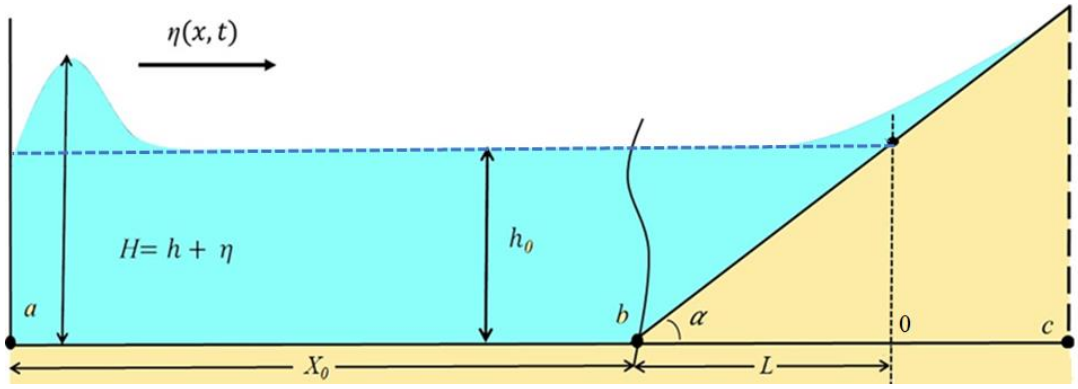

Figure 1: Bathymetry sketch Bathymetry sketch of numerical simulations and analytical solution. The blue dots line corresponding to the still water level. The wavy line regards analytical solution, which does not take into account the merging between constant depth and beach slope.

To do this we represent the input wave η_{X0} as a Fourier integral:

$$\eta_{X0} = \int_{-\infty}^{+\infty} B(\omega)\exp(i\omega t)\,d\omega\,. \tag{6}$$

Its complex spectrum $B(\omega)$ can be found in an explicit form in terms of the inverse Fourier transform:

$$B(\omega) = \frac{1}{2\pi}\int_{-\infty}^{+\infty} \eta_{X0}(t)\exp(-i\omega t)\,dt\,. \tag{7}$$

Eq. (7) can be re-written in terms of the water displacement, produced by the wave maker at the left boundary (Zahibo et al. 2008):

$$B(\omega) = \frac{1}{2\pi i\omega}\int_{-\infty}^{+\infty} \frac{d\eta_0}{dz}\exp\left(-i\omega\left[z + \frac{x + X_0 + L}{V(\eta_0)}\right]\right)dz\,, \qquad z = t - \frac{x + X_0 + L}{V(\eta_0)}\,. \tag{8}$$

In this study we consider long single pulses of positive polarity:

$$\eta_0(t) = A\,\mathrm{sech}^2\left(\frac{t}{T}\right), \tag{9}$$

where A is the input wave height and T is the wave period at the location with the water depth h_0. The wave described by Eq. (9) has an arbitrary height and period and, therefore, does not satisfy properties of the soliton, but just has a sech^2 shape. Substituting Eq. (9) into Eq. (8), we can calculate the complex spectrum $B(\omega)$.

Wave run-up oscillations at the coast $r(t)$ and the velocity of the moving shoreline $u(t)$ can be found from (Didenkulova et al. 2008):

https://doi.org/10.5194/nhess-2019-182
Preprint. Discussion started: 20 June 2019

Natural Hazards and Earth System Sciences
Discussions

$$r(t) = R\left(t + \frac{u}{g\tan\alpha}\right) - \frac{u^2}{2g}, \tag{10}$$

$$u(t) = U\left(t + \frac{u(t)}{g\tan\alpha}\right), \tag{11}$$

$$R(t) = \sqrt{2\pi\tau(L)}\int_{-\infty}^{+\infty}\sqrt{|\omega|}H(\omega)\exp\left\{i\left(\omega\left(t-\tau(L)\right)+\frac{\pi}{4}\mathrm{sign}(\omega)\right)\right\}d\omega, \tag{12}$$

$$U(t) = \frac{1}{\tan\alpha}\frac{dR}{dt}, \tag{13}$$

where $\tau = 2L/\sqrt{gh_0}$ is a travel time to the coast.

This solution we also compare with the run-up of a single wave of positive polarity described by Eq. (9) (without nonlinear deformation). The maximum run-up height $R_{\max}$ of such wave (9) can be found from (Didenkulova et al. 2008; Sriram et al. 2016):

$$\frac{R_{\max}}{A} = 2.8312\sqrt{\cot\alpha}\left(\frac{1}{gh_0}\left(\frac{2h_0}{\sqrt{3T}}\right)^2\right)^{1/4} \tag{14}$$

If the initial wave is soliton, Eq. (14) coincides with the famous Synolakis formula (Synolakis, 1987).

Numerical model

Numerically, we solve the nonlinear shallow water equations Eqs. (1),(2) written in a conservative form for a total water depth. We include the effect of the varying bathymetry (in space) and neglect all friction effects. However, the resulting numerical model will take into account for some dissipation thanks to the numerical dissipation, which is absolutely necessary for the stability of the scheme and should not influence much run-up characteristics. Namely, we employ the natural numerical method, which was developed especially for conservation laws - the finite volume schemes.

The numerical scheme is based on the second order in space UNO2 reconstruction, which is briefly described in (Dutykh et al. 2011b). In time we employ the third order Runge-Kutta scheme with locally adaptive time steps in order to satisfy the CFL stability condition. The numerical technique to simulate the wave run-up was described previously in (Dutykh et al. 2011a). The bathymetry source term is discretized using the hydrostatic reconstruction technique, which implies the well-balanced property of the numerical scheme (Gosse, 2013).

https://doi.org/10.5194/nhess-2019-182
Preprint. Discussion started: 20 June 2019

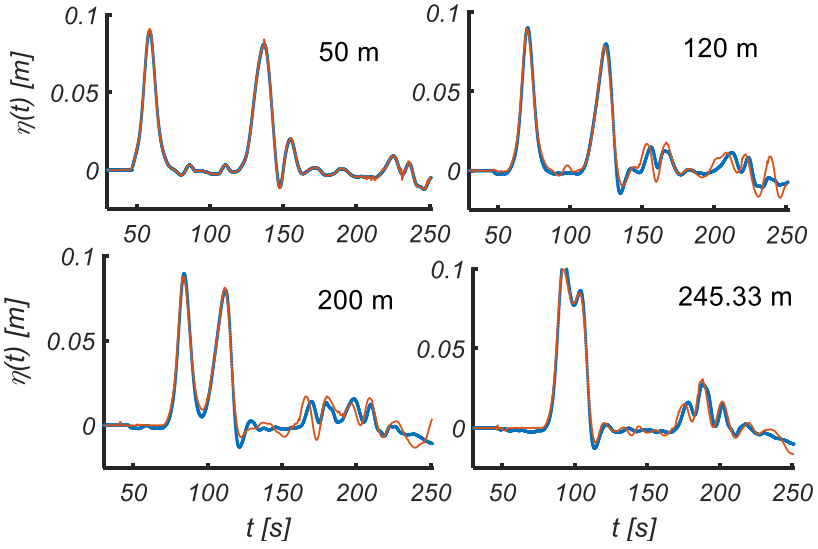

Figure 2: Water elevations along the 251 m long constant depth section of the Large Wave Flume (GWK), h_0 = 3.5 m, A = 0.1 m, T = 20 s, tanα = 1:6: results of numerical simulation are shown with red line, and experimental data are shown with the blue line.

The numerical scheme is validated against experimental data of wave propagation and run-up in the Large Wave Flume (GWK), Hannover, Germany. The experiments were set with a flat bottom with constant depth h0 = 3.5 m and length [a, b] = 251 m, and a plane beach with a slope tanα = 1:6 (see Fig. 1). The flume had 16 wave gauges along the constant depth section and a run-up gauge on the slope. The incident wave had amplitude, A = 0.1 m, and period, T = 20 s. The detailed description of the experiments can be found in Didenkulova et al (2013). The results of numerical simulations are in a good agreement with the laboratory experiments as along the constant depth section (see Fig. 2) as also on the beach (Fig. 3). The comparison of run-up height calculated numerically and analytically using the approach described in Section 2 with the experimental record in shown in Fig. 3. It can be seen that the experimentally recorded wave is slightly smaller which may be caused by the bottom friction and especially on the slope. Both numerical and analytical models describe the first wave of positive polarity rather well. The numerical prediction of run-up height is slightly higher than the analytical one. This additional increase in the run-up height in numerical model may be explained by the nonlinear interaction with the reflected wave, which is not taken into account in the analytical model. The wave of negative polarity is much more sensitive to all the effects mentioned above than the wave of positive polarity and, therefore, looks different for all three lines in Fig. 3. By introducing additional dissipation in numerical model one can easily reach perfect agreement between the numerical simulations and experimental data. However, we do not do so, since below we are focusing on the analysis of analytical results and for clarity would like to avoid additional parameters in the numerical model. Also, we focus on the maximum run-up height and, therefore, expect small differences between the results of analytical and numerical models.

https://doi.org/10.5194/nhess-2019-182
Preprint. Discussion started: 20 June 2019

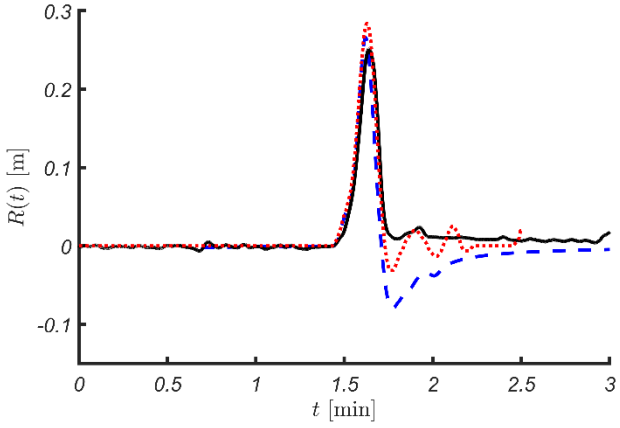

Figure 3: Run-up height of the long single wave with A = 0.1 m and T = 20 s on a beach slope tanα = 1:6, the numerical solution is shown with the red dots line, analytical solution is shown with blue dashed line and the experimental record is shown with the black solid line.

4. Results of numerical and analytical calculations

It is reported in (Didenkulova et al 2007; Didenkulova 2009) for a periodic sine wave, that the extreme run-up height increases proportionally to the square root of the wave front steepness. In this section, we study the nonlinear deformation and steepening of waves described by Eq. (9) and its effect on the extreme wave run-up height. The corresponding bathymetries used in analytical and numerical calculations are shown in Fig. 1. The water depth in the section of constant depth h_0 is kept 3.5 m for all simulations. The input wave parameters such as wave amplitude, A, and wave period, T, are changed as well as the parameters of the bathymetry i.e. the length of the constant depth section, X_0. The beach slope is taken tanα = 1:20 for all simulations.

We underline that in order to have analytical solution, the criterion of no wave breaking should be satisfied. Therefore, all analytical and numerical calculations below are chosen for non-breaking waves.

Fig. 4 shows the maximum run-up height, R_{max} as a function of the initial wave amplitude, A for different distances to the bottom slope, X_0 = 100 m, 200 m, 300 m, 400 m. Analytical solution described in Section 2 is shown with lines and numerical solution described in Section 3 is shown with symbols (diamonds, triangles, squares and circles). The period of the initial wave is taken T = 10 s. It can be seen that in most cases and especially for small values of X_0 = 100 m and 200 m, numerical simulations give larger run-up heights than analytical predictions. These differences can be explained by the effects of wave reflection from the underwater beach slope, which are not taken into account in the analytical solution. For larger distances X_0 = 400 m, both analytical and numerical solutions give similar results, supported by the numerical dissipation in the numerical code. It should be mentioned that we use zero dissipation rate for these simulations, however, small dissipation for stability of the scheme is still needed and this may become noticeable at large distances. During sech^2-

https://doi.org/10.5194/nhess-2019-182
Preprint. Discussion started: 20 June 2019

Natural Hazards and Earth System Sciences
Discussions

shaped wave (A = 0.1 m, T = 10 s) propagation over a 500 m long section of constant depth h_0 = 3.5 m, the reduction of initial wave amplitude constitutes 2 mm, that is ~2 %.

It is worth mentioning, that for small initial wave amplitudes all run-up heights are close to each other and are close to the thick black line which corresponds to Eq. (14) for wave run-up on a beach without constant depth section. This means that the effects we are talking about are important only for nonlinear waves and irrelevant for weakly nonlinear or almost linear waves.

The same effects can be seen in Fig. 5, which shows the maximum run-up height, R_{max} as a function of distance to the slope, X_0 for different amplitudes of the initial wave, A. The period of the initial wave remain the same as in Fig. 4. The distance X_0 changes from 50 m to 550 m. the analytical solution is shown with lines while the numerical solution is shown with symbols (triangles, squares and circles).It can be seen in Fig. 5, for smaller values of X_0 (i.e. 100 m, 200 m and 300 m) numerical predictions provide relatively larger run-up values, as compared with analytical predictions, while for higher values of X_0 (i.e. 400m and 500 m) the differences are significantly reduced. A relevant change of this behaviour is given for A = 0.2 m. We can observe that numerical predictions for this amplitude become smaller than analytical predictions for X_0 > 500 m. As stated above, we believe that this can be a result of interplay of two effects: reflection from the underwater bottom slope, which is not taken into account in the analytical prediction and the numerical dissipation, which affect the numerical results.

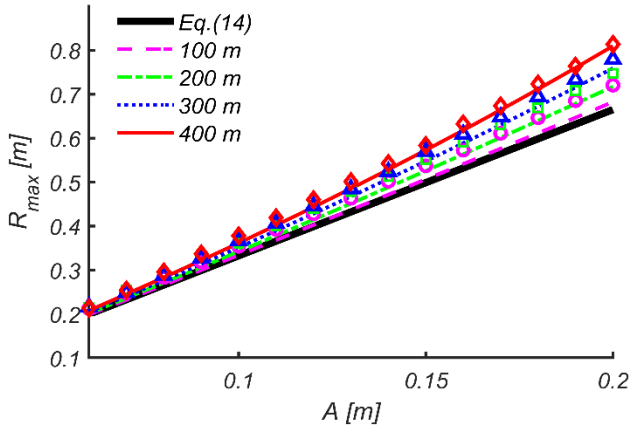

Figure 4: Maximum run-up height, R_{max} as a function of initial wave amplitude, A, for different distances to the slope, X_0. Analytical solution described in Section 2 is shown with lines and numerical solution described in Section 3 is shown with symbols (diamonds, triangles, squares and circles) with matching colours. The thick black line corresponds to Eq. (14) for wave run-up on a beach without constant depth section. The period of the initial wave is taken T = 10 s.

https://doi.org/10.5194/nhess-2019-182
Preprint. Discussion started: 20 June 2019

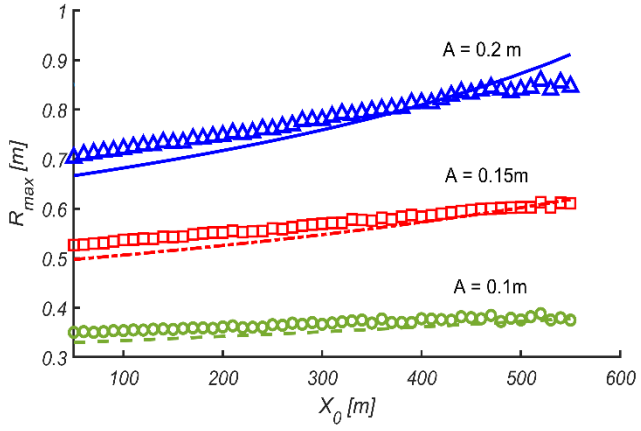

Figure 5: Maximum run-up height, R_{max} as a function of distance to the slope, X_0 for different amplitudes of the initial wave, A. Analytical solution described in Section 2 is shown with lines and numerical solution described in Section 3 is shown with symbols (triangles, squares and circles) with matching colours. The period of the initial wave is taken T = 10 s.

The dependence of maximum run-up height, R_{max} on the period of the initial wave is shown in Fig. 6. It can be seen that the difference between numerical and analytical results increases with an increase in wave periods. We relate this effect with wave reflections from the slope, which are not properly accounted in our analytical approach. As one can see from Fig. 7, this difference for a milder beach slope tanα = 1:50 is reduced.

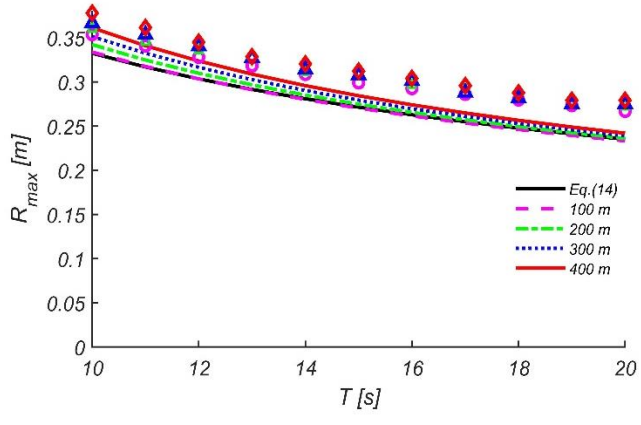

Figure 6: Maximum run-up height, R_{max} as a function of initial wave period, T, for different distances to the slope, X_0. Analytical solution described in Section 2 is shown with lines and numerical solution described in Section 3 is shown with symbols (diamonds, triangles, squares and circles) with matching colours. The thick black line corresponds to Eq. (14) for wave run-up on a beach without constant depth section. The amplitude of the initial wave is taken A = 0.1 m.

https://doi.org/10.5194/nhess-2019-182
Preprint. Discussion started: 20 June 2019

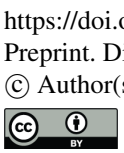

Natural Hazards and Earth System Sciences
Discussions

The next Fig. 8 supports all the conclusions drawn above. It also shows that difference between analytical and numerical results increases with an increase in wave period. As pointed out before for small wave periods the numerical solution may coincide with the analytical one as happens for T = 10 s or even become smaller.

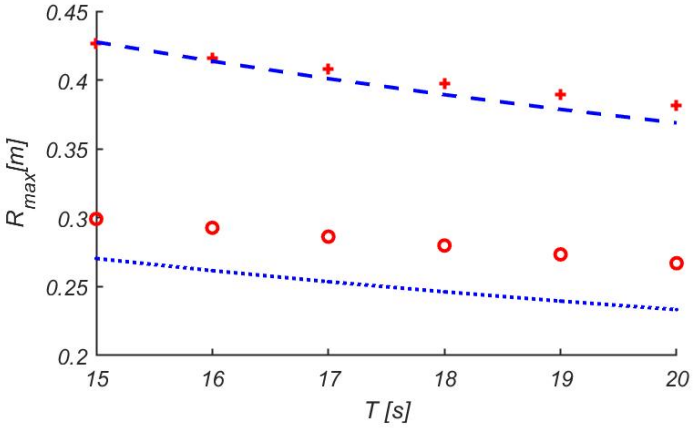

Figure 7: Maximum run-up height, R_{max} as a function of initial wave period, T, for X_0 = 100 m. Analytical solutions for tanα = 1:20 and tanα = 1:50 are shown with dotted and dashed lines respectively, while numerical simulations for tanα = 1:20 and tanα = 1:50 are shown with circles and crosses respectively. The amplitude of the initial wave is taken A = 0.1 m.

Important, that both analytical and numerical results in Fig. 5 and Fig. 8 demonstrate an increase in maximum run-up height with an increase in the distance X_0. This result is in agreement with the conclusions of (Didenkulova et al 2007; Didenkulova, 2009) for sinusoidal waves. In order to be consistent with the results of (Didenkulova et al 2007; Didenkulova, 2009), we connect the distance X_0 with the incident wave front steepness in the beginning of the bottom slope. The wave front steepness s is defined as maximum of the time derivative of water displacement $d\eta/dt$, and is studied in relation with the initial wave front steepness, s_0, where:

$$s(x) = \max\left(d\eta(x,t)/dt\right), \qquad s_0 = \max\left(d\eta(x=a,t)/dt\right), \tag{15}$$

In order to calculate the incident wave front steepness in the beginning of the bottom slope from results of numerical simulations we should separate the incident wave and the wave reflected from the bottom slope. At the same time the wave steepening along the basin of constant depth is very well described analytically as demonstrated in Fig. 9.

It can be seen that the wave transformation described by the analytical model is in a good agreement with numerical simulations. Therefore, below we reference to the analytically defined wave front steepness having in mind that it well coincides with the numerical one. Having said this, we approach the main result of this paper which is shown in Fig. 10. The analytical prediction is given by the red solid line. It is universal for single waves of positive polarity in different amplitudes and periods and can be well approximated by the power fit (coefficient of determination R-squared = 0.99):

https://doi.org/10.5194/nhess-2019-182
Preprint. Discussion started: 20 June 2019

Natural Hazards and Earth System Sciences
Discussions

$$R_{\max}/R_0 = \left(s/s_0\right)^{0.42}, \tag{16}$$

where $R_{\max}$ is the maximum run-up height in the conjoined basin, R_0 the maximum run-up height on a plane beach.

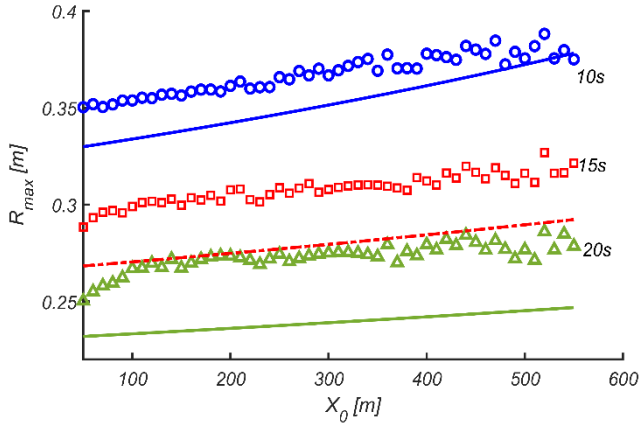

Figure 8: Maximum run-up height, $R_{\max}$ as a function of distance to the slope, X_0 for different initial wave periods, T. Analytical solution described in Section 2 is shown with lines and numerical solution described in Section 3 is shown with symbols (triangles, squares and circles) with matching colors. The amplitude of the initial wave is taken A = 0.1 m.

The fit is shown in Fig. 10 by the black dashed line. For comparison, the dependence of the maximum run-up height on the wave front steepness obtained using the same method for a sine wave is stronger than for a single wave of positive polarity (Didenkulova et al. 2007) and is proportional to the square root of the wave front steepness. This is logical as sinusoidal wave has a sign-variable form and, therefore, excites a higher run-up. For possible mechanisms, see discussion on *N*-waves in (Tadepalli and Synolakis 1994).

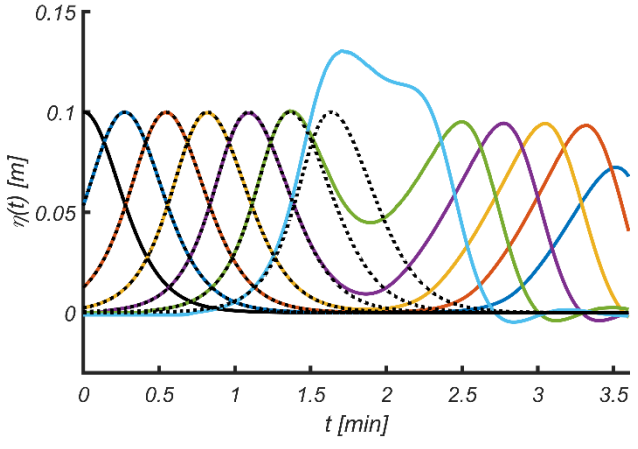

https://doi.org/10.5194/nhess-2019-182
Preprint. Discussion started: 20 June 2019

Natural Hazards and Earth System Sciences
Discussions

Figure 9: Wave evolution at different locations x = 0 m, 100 m, 200 m, 300 m, 400 m, 500 m and 600 m along the section of constant depth for a basin with X_0 = 600 m and tanα = 1:20. Numerical results are shown with solid lines, while the analytical predictions are given by the black dotted lines. The parameters of the wave: A = 0.1 m, T = 20 s.

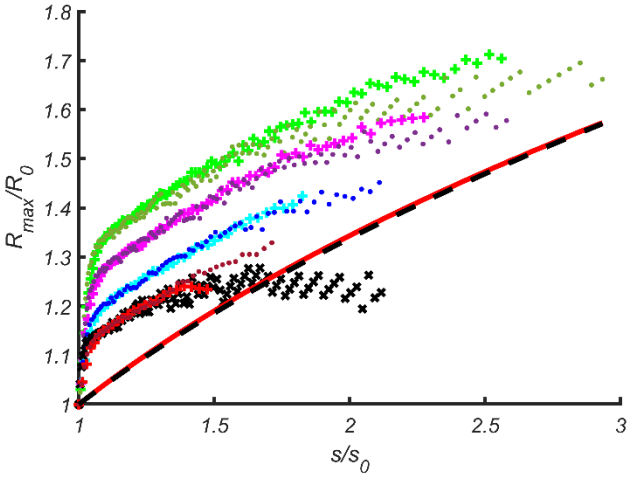

Figure 10: Maximum run-up height in the conjoined basin, R_{max}, normalized by the maximum run-up height on a plane beach, R_0 versus the wave front steepness for different wave amplitudes and periods: A = 0.1 m, T = 10 s (black crosses), A = 0.2 m, T = 10 s (brown points), A = 0.3 m, T = 10 s (red plus signs), A = 0.2 m, T = 13 s (blue points), A = 0.3 m, T = 13 s (turquoise plus signs), A = 0.2 m, T = 17 s (violet points), A = 0.3 m, T = 17 s (pink plus signs), A = 0.2 m, T = 20 s (dark green points), A = 0.3 m, T = 20 s (light green plus signs). All markers correspond to the results of numerical simulations, while the asymptotic analytical predictions are given by the red solid line. Black dashed line correspond to the power fit of the analytical results Eq. (20).

The results of numerical simulations are shown in Fig. 10 with different markers. First, it can be seen that all numerical curves are somehow parallel to the analytical one. Second, numerical data for the same period, but different amplitudes follow the same curve. The run-up is higher for waves with longer periods.

5. Conclusion

In this paper, we study the nonlinear deformation and run-up of tsunami waves, represented by single waves of positive polarity. We consider the conjoined water basin, which consists of a section of constant depth and a plane beach. While propagating in such basin, the wave shape changes forming a steep front. Tsunamis often approach the coast with a steep wave front, as it was observed during large tsunami events, e.g. 2004 Indian Ocean Tsunami and 2011 Tohoku tsunami.

The study is performed both analytically and numerically in the framework of the nonlinear shallow water theory. The analytical solution considers nonlinear wave steepening in the constant depth section and wave run-up on a plane beach independently and, therefore, does not take into account wave reflection from the bottom slope. The propagation along the bottom of constant depth is described by Riemann wave, while the wave run-up on a plane beach is calculated using rigorous analytical solutions of the nonlinear shallow water theory following the Carrier-Greenspan approach. The numerical scheme

https://doi.org/10.5194/nhess-2019-182
Preprint. Discussion started: 20 June 2019

employs the finite volume method and is based on the second order UNO2 reconstruction in space and the third order Runge-Kutta scheme with locally adaptive time steps. The model is validated against experimental data.

Found analytically, that maximum tsunami run-up height on a beach depends on the wave front steepness at the toe of the bottom slope. This dependence is general for single waves of different amplitudes and periods and can be approximated by the power fit: $R_{\max} / R_0 = \left(s / s_0\right)^{0.42}$.

This dependence is slightly weaker than the corresponding dependence for a sine wave, proportional to the square root of the wave front steepness (Didenkulova et al. 2007). The stronger dependence of a sine wave run-up on the wave front steepness is consistent with the philosophy of *N*-waves (Tadepalli and Synolakis 1994).

Shown numerically, that all numerical curves for different wave amplitudes and periods, are parallel to the analytical one. Therefore, for estimates one can use the analytical dependence on the wave front steepness.

Acknowledgements

The authors are very grateful to Professor Efim Pelinovsky, who gave an idea to this study a few years ago. The analytical calculations were performed with the support of RSF grant 16-17-00041. The numerical simulations and its comparison with the analytical findings were supported by the ETAG grant PUT1378. Authors also thank the PHC PARROT project No 37456YM, which funded the authors' visits to France and Estonia and allowed this collaboration.

References

Brocchini, M., and Gentile, R.: Modelling the run-up of significant wave groups, Continental Shelf Research, 21(15), 1533-1550, https://doi.org/10.1016/S0278-4343(01)00015-2, 2001.

Carrier, G. F., and Greenspan, H. P.: Water waves of finite amplitude on a sloping beach, Journal of Fluid Mechanics, 4(1), 97-109, https://doi.org/10.1017/S0022112058000331, 1958.

Carrier, G.F., Wu, T.T., and Yeh, H.: Tsunami run-up and draw-down on a plane beach, Journal of Fluid Mechanics, 475, 79-99, https://doi.org/10.1017/S0022112002002653, 2003.

Didenkulova, I.: New trends in the analytical theory of long sea wave runup, in: Applied Wave Mathematics, edited by: Quak E., Soomere T., Springer, Berlin, Heidelberg, Germany, 265-296, https://doi.org/10.1007/978-3-642-00585-5_14, 2009.

Didenkulova, I., Denissenko, P., Rodin, A., and Pelinovsky, E.: Effect of asymmetry of incident wave on the maximum runup height, Journal of Coastal Research, 65(1), 207-212, https://doi.org/10.2112/SI65-036.1, 2013.

Didenkulova, I., Pelinovsky, E.N., and Didenkulova, O.I.: Run-up of long solitary waves of different polarities on a plane beach. Izvestiya, Atmospheric and Oceanic Physics, 50(5), 532-538, https://doi.org/10.1134/S000143381405003X, 2014.

Didenkulova, I., Pelinovsky, E. and Soomere, T.: Runup characteristics of symmetrical solitary tsunami waves of "unknown" shapes, Pure and Applied Geophysics, 165 (11/12), 2249-2264, https://doi.org/10.1007/978-3-0346-0057-6_13, 2008.

https://doi.org/10.5194/nhess-2019-182
Preprint. Discussion started: 20 June 2019

Didenkulova, I., Pelinovsky, E., Soomere, T., and Zahibo, N.: Run-up of nonlinear asymmetric waves on a plane beach, in: Tsunami and nonlinear waves, edited by: Kundu A., Springer, Berlin, Heidelberg, Germany, 175-190, https://doi.org/10.1007/978-3-540-71256-5_8, 2007.

Dutykh, D., Poncet, R. and Dias, F.: The VOLNA code for the numerical modeling of tsunami waves: Generation, propagation and inundation, European Journal of Mechanics-B/Fluids, 30(6), 598-615, https://doi.org/10.1016/j.euromechflu.2011.05.005, 2011a.

Dutykh, D., Katsaounis, T., and Mitsotakis, D.: Finite volume schemes for dispersive wave propagation and runup, Journal of Computational Physics, 230(8), 3035-3061, https://doi.org/10.1016/j.jcp.2011.01.003, 2011b.

Fuhrman, D.R., and Madsen, P.A.: Simulation of nonlinear wave run-up with a high-order Boussinesq model, Coastal Engineering, 55(2), 139-154, https://doi.org/10.1016/j.coastaleng.2007.09.006, 2008.

Gosse, L.: Computing Qualitatively Correct Approximations of Balance Laws: Exponential-Fit, Well-Balanced and Asymptotic-Preserving, Springer Milan, Italy, 2013.

Hubbard, M.E., and Dodd, N.: A 2D numerical model of wave run-up and overtopping, Coastal Engineering, 47(1), 1-26, https://doi.org/10.1016/S0378-3839(02)00094-7, 2002.

Kânoğlu, U.: Nonlinear evolution and runup–rundown of long waves over a sloping beach, Journal of Fluid Mechanics, 513, 363-372, https://doi.org/10.1017/S002211200400970X, 2004.

Kânoğlu, U., and Synolakis, C.: Initial value problem solution of nonlinear shallow water-wave equations, Physical Review Letters, 97(14), 148501, https://doi.org/10.1103/PhysRevLett.97.148501, 2006.

Keller, J.B., and Keller, H.B.: Water wave run-up on a beach, Service Bureau Corp, New York, 1964.

Li, Y., and Raichlen, F.: Non-breaking and breaking solitary wave run-up, Journal of Fluid Mechanics, 456, 295-318, https://doi.org/10.1017/S0022112001007625, 2002.

Lin, P., Chang, K.A., and Liu, P.L.F.: Runup and rundown of solitary waves on sloping beaches, Journal of Waterway, Port, Coastal, and Ocean Engineering, 125(5), 247-255, https://doi.org/10.1061/(ASCE)0733-950X(1999)125:5(247), 1999.

Madsen, P.A., and Fuhrman, D.R.: Run-up of tsunamis and long waves in terms of surf-similarity, Coastal Engineering, 55(3), 209-223, https://doi.org/10.1016/j.coastaleng.2007.09.007, 2008.

Madsen, P.A., Fuhrman, D.R., and Schäffer, H.A.: On the solitary wave paradigm for tsunamis, Journal of Geophysical Research: Oceans, 113 (C12), 1-22, https://doi.org/10.1029/2008JC004932, 2008.

Madsen, P. A., and Schaeffer, H. A.: Analytical solutions for tsunami run-up on a plane beach: single waves, N-waves and transient waves, Journal of Fluid Mechanics, 645, 27-57, https://doi.org/10.1017/S0022112009992485, 2010.

Mazova, R.K., Osipenko, N.N., and Pelinovsky, E.N.: Solitary wave climbing a beach without breaking, Rozprawy Hydrotechniczne, 54, 71-80, 1991.

Mei, C.C. The applied dynamics of ocean surface waves, World Scientific, Singapore, 1989.

McGovern, D.J., Robinson, T., Chandler, I.D., Allsop, W., and Rossetto, T.: Pneumatic long-wave generation of tsunami-length waveforms and their runup, Coastal Engineering, 138, 80-97, https://doi.org/10.1016/j.coastaleng.2018.04.006, 2018.

Pedersen, G., and Gjevik, B.: Run-up of solitary waves, Journal of Fluid Mechanics, 135, 283-299, https://doi.org/10.1017/S002211208700329X, 1983.

Pelinovsky, E.N., and Mazova, R.K.: Exact analytical solutions of nonlinear problems of tsunami wave run-up on slopes with different profiles, Natural Hazards, 6(3), 227-249, https://doi.org/10.1007/BF00129510, 1992.

https://doi.org/10.5194/nhess-2019-182
Preprint. Discussion started: 20 June 2019

Natural Hazards and Earth System Sciences
Discussions

Raz, A., Nicolsky, D., Rybkin, A. and Pelinovsky E.: Long wave runup in asymmetric bays and in fjords with two separate heads, Journal of Geophysical Research: Oceans, 123(3), 2066-2080, https://doi.org/10.1002/2017JC013100, 2018.

Sriram, V., Didenkulova, I., Sergeeva, A., and Schimmels, S.: Tsunami evolution and run-up in a large scale experimental facility, Coastal Engineering, 111, 1-12, https://doi.org/10.1016/j.coastaleng.2015.11.006, 2016.

Schimmels, S., Sriram, V., and Didenkulova, I.: Tsunami generation in a large scale experimental facility, Coastal Engineering, 110, 32-41, https://doi.org/10.1016/j.coastaleng.2015.12.005, 2016.

Stoker, J.J.: Water waves, the mathematical theory with applications, Interscience Publishers Inc., New York, 1957.

Synolakis, C. E.: The run-up of solitary waves, Journal of Fluid Mechanics, 185, 523-545, https://doi.org/10.1017/S002211208700329X, 1987.

Synolakis, C.E., Deb, M.K., and Skjelbreia, J.E.: The anomalous behavior of the runup of cnoidal waves, Physics of Fluids, 31(1), 3-5, https://doi.org/10.1063/1.866575, 1988.

Tadepalli, S., and Synolakis, C.E.: The run-up of N-waves, Proc. Roy. Soc, London A, 445, 99–112, https://doi.org/10.1098/rspa.1994.0050, 1994.

Tang, J., Shen, Y., Causon, D.M., Qian, L. and Mingham, C.G.: Numerical study of periodic long wave run-up on a rigid vegetation sloping beach, Coastal Engineering, 121, 158-166, https://doi.org/10.1016/j.coastaleng.2016.12.004, 2017.

Tinti, S., and Tonini, R.: Analytical evolution of tsunamis induced by near-shore earthquakes on a constant-slope ocean, Journal of Fluid Mechanics, 535, 33-64, https://doi.org/10.1017/S0022112005004532, 2005.

Touhami, H.E. and Khellaf, M.C.: Laboratory study on effects of submerged obstacles on tsunami wave and run-up, Natural Hazards, 87(2), 757-771, https://doi.org/10.1007/s11069-017-2791-9, 2017.

Yao, Y., He, F., Tang, Z. and Liu, Z.: A study of tsunami-like solitary wave transformation and run-up over fringing reefs, Ocean Engineering, 149, 142-155, https://doi.org/10.1016/j.oceaneng.2017.12.020, 2018.

Zahibo, N., Didenkulova, I., Kurkin, A. and Pelinovsky E.: Steepness and spectrum of nonlinear deformed shallow water wave, Ocean Engineering, 35 (1), 47–52, https://doi.org/10.1016/j.oceaneng.2007.07.001, 2008.

Zainali, A., Marivela, R., Weiss, R., Yang, Y. and Irish, J.L.: Numerical simulation of nonlinear long waves in the presence of discontinuous coastal vegetation, Marine Geology, 396, 142-149, https://doi.org/10.1016/j.margeo.2017.08.001, 2017.